Substrate reduction reduces gangliosides in postnatal cerebrum-brainstem and cerebellum in GM1 gangliosidosis mice

J. L. Kasperzyk, A. d'Azzo, F. M. Platt, J. Alroy, and T. N. Seyfried[1]

Department of Biology, Boston College, Chestnut Hill, MA 02467

Abstract **II^{3}NeuAc-GgOse$_4$Cer (GM1) gangliosidosis is an incurable lysosomal storage disease caused by a deficiency in acid β-galactosidase (β-gal), resulting in the accumulation of ganglioside GM1 and its asialo derivative GgOse$_4$Cer (GA1) in the central nervous system, primarily in the brain. In this study, we investigated the effects of *N*-butyldeoxygalacto-nojirimycin (*N*B-DGJ), an imino sugar that inhibits ganglioside biosynthesis, in normal C57BL/6J mice and in β-gal knockout (β-gal$^{-/-}$) mice from postnatal day 9 (p-9) to p-15. This is a period of active cerebellar development and central nervous system (CNS) myelinogenesis in the mouse and would be comparable to late-stage embryonic and early neonatal development in humans. *N*B-DGJ significantly reduced total ganglioside and GM1 content in cerebrum-brainstem (C-BS) and in cerebellum of normal and β-gal$^{-/-}$ mice. *N*B-DGJ had no adverse effects on body weight or C-BS/cerebellar weight, water content, or thickness of the external cerebellar granule cell layer. Sphingomyelin was increased in C-BS and cerebellum, but no changes were found for cerebroside (a myelin-enriched glycosphingolipid), neutral phospholipids, or GA1 in the treated mice. Our findings indicate that the effects of *N*B-DGJ in the postnatal CNS are largely specific to gangliosides and suggest that *N*B-DGJ may be an effective early intervention therapy for GM1 gangliosidosis and other ganglioside storage disorders.**—Kasperzyk, J. L., A. d'Azzo, F. M. Platt, J. Alroy, and T. N. Seyfried. **Substrate reduction reduces gangliosides in postnatal cerebrum-brainstem and cerebellum in GM1 gangliosidosis mice. *J. Lipid Res.* 2005.** 46: **744–751.**

Supplementary key words *N*-butyldeoxygalactonojirimycin • II^3(NeuAc)$_2$-LacCer • II^{3}NeuAc-GgOse$_4$Cer • asialo derivative • myelin • cerebrosides • granule cells • neurodegeneration

GM1 gangliosidosis is an incurable glycosphingolipid (GSL) lysosomal storage disease caused by a genetic deficiency in lysosomal acid β-galactosidase (β-gal) and leads to the storage of II^{3}NeuAc-GgOse$_4$Cer (GM1) and its asialo derivative (GA1) in the central nervous system (CNS) (1). Age of onset ranges from infancy to adulthood, and excessive CNS ganglioside accumulation produces progressive neurodegeneration and brain dysfunction in humans. A β-gal-deficient mouse model of GM1 gangliosidosis was generated using homologous recombination and embryonic stem cell technology (2). We recently showed that these mice accumulate GM1 and GA1 in the brain as early as postnatal day 5 (p-5), thus mimicking the neurochemical features of the infantile disease form (3). In contrast to infantile-onset patients, in whom ganglioside accumulation leads to behavioral and developmental abnormalities within the first few years of life, β-gal-deficient mice are phenotypically indistinguishable from normal mice until adult ages (2).

Most therapies for ganglioside storage diseases focus on augmenting lysosomal enzyme levels and involve bone marrow transplantation, enzyme replacement, stem cell therapy, gene therapy, and chemical chaperone therapy (4–11). These therapeutic approaches, however, have difficulty reducing GSL storage products throughout the CNS. Alternatively, substrate reduction therapy, originally proposed by Radin (12) and others (13–17), aims to reduce GSL synthesis to counterbalance the impaired rate of catabolism, thus reducing GSL accumulation and disease progression. Platt and colleagues (15, 18–21) used this therapy to treat adult-onset ganglioside storage disease in mice more recently. We recently provided evidence that substrate reduction therapy using *N*-butyldeoxygalactonojirimycin (*N*B-DGJ) could significantly reduce total brain ganglioside and GM1 content in neonatal normal and β-gal-deficient mutant mice (3).

The imino sugars *N*-butyldeoxynojirimycin (*N*B-DNJ) and *N*B-DGJ are competitive inhibitors of the ceramide-specific glucosyltransferase that catalyzes the first step in GLS biosynthesis (15). Substrate reduction therapy using *N*B-DNJ and *N*B-DGJ have successfully reduced brain ganglioside content, delayed symptom onset, and increased survival in adult mouse models of the GM2 gangliosidoses (Tay-Sachs disease and Sandhoff disease) (13, 17, 22). *N*B-

Manuscript received 19 April 2004 and in revised form 5 January 2005.

Published, JLR Papers in Press, February 1, 2005.
DOI 10.1194/jlr.M400411-JLR200

[1] To whom correspondence should be addressed.
e-mail: thomas.seyfried@bc.edu

DNJ is also approved for the treatment of type 1 Gaucher disease (glucosylceramide storage) and is under trial evaluation for late-onset Tay-Sachs disease (23–25). *N*B-DGJ, however, may be more suitable for treating neonates than *N*B-DNJ, because digestive abnormalities and weight loss do not occur with *N*B-DGJ treatment (3, 17, 26). Furthermore, we previously showed that *N*B-DGJ could reduce GSL and ganglioside biosynthesis by 90% in normal mouse embryos without impairing viability, growth, or morphogenesis (27). Our studies in embryonic and neonatal mice suggest that *N*B-DGJ may be an effective early intervention therapy for the gangliosidoses.

In this study, we investigated for the first time the effects of *N*B-DGJ in normal C57BL/6J (B6) mice and β-gal-deficient (β-gal$^{-/-}$) mutant mice from p-9 to p-15. This is a period of most active cerebellar development and CNS myelinogenesis in the mouse involving the proliferation and migration of granule cells, synaptogenesis, and the rapid accumulation of cerebroside, a myelin-enriched GSL (28–31) Also, this developmental period is comparable to late-stage embryonic and early development in humans (32, 33). Our results show that *N*B-DGJ significantly reduces cerebrum-brainstem (C-BS) and cerebellar total ganglioside and GM1 content during this critical developmental period. Moreover, no adverse effects of the drug treatment were observed in the normal or mutant mice for cerebellar growth and morphology or brain cerebroside content.

MATERIALS AND METHODS

Mice

The B6 mice were obtained from the Jackson Laboratory (Bar Harbor, ME). B6/129Sv mice, heterozygous for the GM1 gene (β-gal +/−), were obtained from Dr. Alessandra d'Azzo (Saint Jude Children's Research Hospital, Memphis, TN). The B6 mice were used as normal controls because this genetic background largely composed that of the knockout mice. The knockout mice were derived by homologous recombination and recombinant stem cell technology as previously described (2). Homozygous β-gal$^{-/-}$ mouse pups were derived from crossing β-gal$^{-/-}$ adults, thus ensuring that control and drug-treated β-gal$^{-/-}$ pups were compared within the same litter. Likewise, control and drug-treated normal B6 pups were compared within the same litter. Genotypes were determined postmortem by measuring β-gal-specific activity in tail tissue using a modification of the Galjaard procedure (34, 35). All mice were propagated at the Boston College Animal Facility and were housed in plastic cages with filter tops containing Sani-Chip bedding (P. J. Murphy Forest Products Corp., Montville, NJ). The room was maintained at 22°C on a 12 h light/dark cycle. Food (Prolab RMH 3000; PMI LabDiet, Richmond, IN) and water were provided ad libitum. Cotton nesting pads were provided to nursing females for the duration of the experiment. All animal experiments were carried out with ethical committee approval in accordance with the National Institutes of Health Guide for the Care and Use of Laboratory Animals and were approved by the Institutional Animal Care Committee.

*N*B-DGJ treatment and tissue collection

*N*B-DGJ was purchased from Toronto Research Chemicals, Inc. (North York, Ontario, Canada). *N*B-DGJ solutions were prepared in sterile saline to yield a final concentration of ~0.2 mg/μl. Postnatal B6 and β-gal$^{-/-}$ mice were injected daily intraperitoneally from p-9 to p-15 with either vehicle (0.9% saline) or *N*B-DGJ at 600 mg/kg body weight. Injections were performed using a Hamilton syringe (26 gauge, point style 2, 0.5 inch needle length), and volumes ranged from ~10 to 25 μl/mouse. Body weights were measured before cervical dislocation ~4 h after the final injection on p-15. Cerebellum was separated from the C-BS, and the tissues were frozen on dry ice to obtain wet weights. Two or three cerebella were pooled for each B6 sample, but each β-gal$^{-/-}$ cerebellum as well as each C-BS was analyzed separately. The samples were frozen at −80°C and lyophilized to determine water content. Additional mice were killed by CO_2 asphyxiation for histology. The brains of these mice were exposed after midline resection along the sutures of the skull and were immersed in ~25 ml of Bouin's fixative (LabChem, Inc., Pittsburgh, PA) for 3 days at room temperature. The brains were then removed from the skull, placed in diluted Bouin's fixative [1:10 with deionized H_2O (dH_2O)], and stored at 4°C.

Lipid isolation, purification, and quantitation

Total lipid extraction. Total lipids were isolated and purified from the lyophilized brain tissue using modifications of previously described procedures (3, 35, 36). Briefly, total lipids were extracted with 5 ml of $CHCl_3$ and CH_3OH (1:1, v/v) and 0.5 ml of dH_2O. The solution was placed on a magnetic stirrer at room temperature for at least 8 h and then centrifuged for 10 min at 1,200 *g*. The supernatant was removed and the pellet was washed with 2 ml of $CHCl_3/CH_3OH$ (1:1, v/v). The combined supernatants were converted to a $CHCl_3/CH_3OH/dH_2O$ ratio of 30:60:8 (solvent A) by adding 2.5 ml of $CHCl_3$, 8.5 ml of CH_3OH, and 1.6 ml of dH_2O.

Column chromatography. Neutral and acidic lipids were separated using DEAE-Sephadex (A-25; Pharmacia Biotech, Uppsala, Sweden) column chromatography as previously described (37). DEAE-Sephadex was prepared in bulk by washing the resin three times with solvent B ($CHCl_3/CH_3OH$/0.8 M Na acetate, 30:60:8, v/v), equilibrating in solvent B overnight, followed by washing three times with solvent A until neutral. The total lipid extract, suspended in solvent A, was then applied to a DEAE-Sephadex column (1.2 ml bed volume) that had been equilibrated previously with solvent A. The column was washed twice with 20 ml of solvent A, and the entire neutral lipid fraction, consisting of the initial eluent plus washes, was collected. This fraction contained the following lipids: cholesterol, phosphatidylcholine, phosphatidylethanolamine, plasmalogens, ceramide, sphingomyelin, cerebrosides, and GA1. Next, acidic lipids were eluted from the column with 30 ml of solvent B. This fraction contained the gangliosides and other less hydrophilic acidic lipids.

Ganglioside purification. The acidic lipid fraction containing gangliosides was dried by rotary evaporation and transferred to a 15 ml graduated glass conical tube using $CHCl_3/CH_3OH$ (1:1, v/v) and adjusted to 7 ml using the same solvent. Water (2.6 ml) was added and the mixture was inverted, vortexed, and centrifuged for ~10 min at 1,200 *g* to partition gangliosides into the upper phase (36, 38). The upper aqueous phase was removed and the lower organic phase was washed once with 4.5 ml of the Folch pure solvent upper phase ($CHCl_3/CH_3OH/dH_2O$, 3:48:47, v/v). The combined upper phases, containing the gangliosides, were adjusted to 11 ml using the pure solvent upper phase.

Resorcinol assay. An aliquot of the ganglioside fraction (Folch upper phase) was evaporated under a stream of nitrogen and analyzed for sialic acid content using a modified resorcinol method (39–41). *N*-acetylneuraminic acid (Sigma, St. Louis, MO) was used as an external standard. Samples were dissolved in 1 ml of resorcinol reagent/dH_2O (1:1, v/v), boiled for 15 min, and then

cooled in an ice bath. Butyl acetate/1-butanol (1.5 ml; 85:15, v/v) was then added, and the samples were vortexed and centrifuged at 1,200 *g*. The violet supernatant was removed and analyzed at 580 nm in the Shimadzu UV-1601 ultraviolet-visible spectrophotometer (Shimadzu, Kyoto, Japan).

Base treatment and desalting. After removing the aliquots for the resorcinol assay, the ganglioside fraction was evaporated under a stream of nitrogen and treated with mild base (1 ml of 0.5 M NaOH) in a shaking water bath at 37°C for 1.5 h. Base and salts were separated from the gangliosides using a modification of a previously described method (42). The sample was applied to a C18 reverse-phase Bond Elute column (Varian, Harbor City, CA) that was equilibrated with 5 ml each of $CHCl_3/CH_3OH$ (1:1, v/v), $CHCl_3$, and 0.1 M NaCl. The column was washed with 25 ml of dH_2O to remove salts. Gangliosides were eluted from the column with 2 ml of $CHCl_3$ followed by 4 ml of $CHCl_3/CH_3OH$ (1:1, v/v) and stored at 4°C.

Neutral lipid purification. Neutral lipids were dried by rotary evaporation and resuspended in 10 ml of $CHCl_3/CH_3OH$ (2:1, v/v). To further purify GA1, a 4 ml aliquot of the neutral lipid fraction was evaporated under a stream of nitrogen, base treated, and Folch partitioned as described previously and above (3). The Folch lower phase containing GA1 was evaporated under a stream of nitrogen and resuspended in 10 ml of $CHCl_3/CH_3OH$ (2:1, v/v).

High-performance thin-layer chromatography. All lipids were analyzed qualitatively by high-performance thin-layer chromatography (HPTLC) according to previously described methods (36, 37, 43). Lipids were spotted on 10 × 20 cm Silica gel 60 HPTLC plates (E. Merck, Darmstadt, Germany) using a Camag Linomat III auto-TLC spotter (Camag Scientific, Inc., Wilmington, NC). The amount of lipid per lane was equivalent to 1.5 μg of total sialic acid for gangliosides and either 0.4 or 0.3 mg of tissue dry weight for GA1 or neutral lipids, respectively. To enhance precision, an internal standard (oleoyl alcohol) was added to the neutral lipid standards and samples as previously described (37). Purified lipid standards were either purchased from Matreya, Inc. (Pleasant Gap, PA), or Sigma or were a gift from Dr. Robert Yu (Medical College of Georgia, Augusta, GA).

For gangliosides and GA1, the HPTLC plates were developed by a single ascending run with $CHCl_3/CH_3OH/dH_2O$ (55:45:10, v/v for gangliosides; 65:35:8, v/v for GA1) containing 0.02% $CaCl_2{\cdot}2H_2O$. The plates were sprayed with either the resorcinol-HCl reagent or the orcinol-H_2SO_4 reagent and heated at 95°C for 30 min to visualize gangliosides or GA1, respectively (39, 44). For neutral lipids, the plates were developed to a height of 4.5 cm with chloroform-methanol-acetic acid-formic acid-water (35:15:6:2:1, v/v), dried for ~20 min, and developed to the top with hexanes-diisopropyl ether-acetic acid (65:35:2, v/v) as previously described (37, 45). Neutral lipids were visualized by charring with 3% cupric acetate in 8% phosphoric acid solution, followed by heating in an oven at 160–170°C for 7 min.

The percentage distribution and density of the individual bands was determined by scanning the plates on a Personal Densitometer SI with ImageQuant software (Molecular Dynamics, Sunnyvale, CA) for gangliosides and neutral lipids or on a ScanMaker 4800 with ScanWizard5 V7.00 software (Microtek, Carson, CA) for GA1. The total brain ganglioside distribution was normalized to 100%, and the percentage distribution values were used to calculate sialic acid concentration (micrograms of sialic acid per 100 mg dry weight) of individual gangliosides as we previously described (46). The density values for GA1 and sphingomyelin were fit to a standard curve of the respective lipid and used to calculate individual concentrations expressed as micrograms per 100 mg dry weight.

Histological analysis. The brains stored in diluted Bouin's fixative were embedded in paraffin, sectioned (sagittal, 5 μm), and stained with hematoxylin and eosin, Luxol Fast Blue (LFB), and Periodic Acid Schiff (PAS) at the Harvard University Rodent Histopathology Core Facility (Boston, MA). Slides were examined using a Zeiss Axioplane 2 imaging universal microscope and a Hamamatsu Orca-ER digital camera with Openlab software. This equipment was also used to measure external granular layer (EGL) thickness in two cerebellar regions (vernal lobules VI and X) on hematoxylin and eosin-stained sections of control and treated β-gal$^{-/-}$ mice. EGL thickness was expressed as the average of 10 measurements per independent sample in which four independent cerebellar samples per group were analyzed.

RESULTS

Our objective was to determine whether substrate reduction therapy using *N*B-DGJ could reduce C-BS and cerebellar ganglioside content in B6 and β-gal$^{-/-}$ mice during a critical period of cerebellar development and myelinogenesis (i.e., from p-9 to p-15). Total ganglioside content was greater in the C-BS than in the cerebellum of both the normal B6 and the mutant mice (**Table 1**). Also, total ganglioside content in the C-BS and the cerebellum was higher in the untreated β-gal$^{-/-}$ mice than in the untreated B6 mice. Daily *N*B-DGJ injections from p-9 to p-15 significantly reduced total C-BS ganglioside content by 16% in the B6 mice and by 19% in the β-gal$^{-/-}$ mice (Table 1). Similarly, *N*B-DGJ reduced total cerebellar ganglioside content by 22% in the B6 mice and by 21% in the β-gal$^{-/-}$ mice (Ta-

TABLE 1. Regional brain ganglioside content in p-15 normal B6 and mutant β-gal$^{-/-}$ mice treated with *N*B-DGJ

			Wet Weight		Water Content		Ganglioside Sialic Acid	
Strain	Treatment[a]	Body Weight	Brain[b]	Cerebellum	Brain	Cerebellum	Brain	Cerebellum
		g	*mg*		%		*μg/100 mg dry wt*	
B6	Control	5.9 ± 0.2 (6)	338.5 ± 2.8 (6)	42.7 ± 0.7 (3)	82.77 ± 0.13 (6)	82.02 ± 0.05 (3)	502 ± 4 (3)	342 ± 13 (3)
	Treated	6.1 ± 0.1 (7)	340.5 ± 2.5 (7)	42.9 ± 0.7 (3)	82.77 ± 0.07 (7)	81.83 ± 0.07 (3)	422 ± 3[c] (3)	266 ± 9[c] (3)
β-Gal$^{-/-}$	Control	8.6 ± 0.5 (3)	361.0 ± 10.4 (3)	51.2 ± 2.0 (3)	82.35 ± 0.04 (3)	81.65 ± 0.09 (3)	587 ± 17 (3)	364 ± 7 (3)
	Treated	8.7 ± 0.1 (3)	350.8 ± 3.6 (3)	50.8 ± 0.9 (3)	82.32 ± 0.15 (3)	82.02 ± 0.13 (3)	478 ± 18[d] (3)	288 ± 5[c] (3)

B6, C57BL/6J; β-gal$^{-/-}$, β-galactosidase knockout; *N*B-DGJ, *N*-butyldeoxygalacto-nojirimycin; p-15, postnatal day 15. Values represent means ± SEM. Numbers in parentheses indicate the number of independent samples analyzed.

[a] Mice were injected daily with either vehicle (control) or *N*B-DGJ (treated) at 600 mg/kg from p-9 to p-15.

[b] Region includes cerebrum + brain stem.

[c] Significantly different from control values at $P < 0.01$ (determined from the two-tailed *t*-test).

[d] Significantly different from control values at $P < 0.05$ (determined from the two-tailed *t*-test).

ble 1). C-BS and cerebellar total ganglioside content was actually lower in the β-gal$^{-/-}$ mice after *N*B-DGJ treatment than in the untreated B6 mice.

The reduction in CNS ganglioside content was not associated with changes in body weight or C-BS/cerebellar weight or water content in either normal or mutant mice (Table 1). The body weight difference between the B6 and the β-gal$^{-/-}$ mice may result from either maternal or strain differences. Furthermore, no differences were found between the control and the treated mice, either B6 or β-gal$^{-/-}$, for eye opening (p-14 to p-15) or righting reflex at p-15. Although C-BS and cerebellar GM1 content was significantly greater in the mutant β-gal$^{-/-}$ mice than in the normal B6 mice, no histological evidence of ganglioside storage material or neuronal vacuoles was seen in the p-15 β-gal$^{-/-}$ mice by light microscopy after LFB staining of paraffin-embedded brain tissue (**Fig. 1**). Also, no ganglioside storage was seen after PAS staining of serial brain sections (data not shown).

The influence of *N*B-DGJ on the qualitative and quantitative distribution of C-BS and cerebellar gangliosides is shown in **Fig. 2** and **Table 2**. Gangliosides that were absent or that constituted less than 1% of the total distribution [GM4, GM3, and GM2 in all regions, and II^3(NeuAc)$_2$-LacCer (GD3) in the β-gal$^{-/-}$ C-BS] were omitted from the computations. In contrast to the C-BS, where GM1 is a major ganglioside, GM1 was a minor ganglioside in the cerebellum of normal B6 mice at p-15 (Table 2). This is consistent with previous observations in normal mice (29, 47). However, GM1 was ~4-fold greater in the C-BS and ~5-fold greater in the cerebellum of the untreated β-gal$^{-/-}$ mice than in the untreated B6 mice (Table 2). *N*B-DGJ significantly reduced C-BS and cerebellar GM1 content by 18% and 17%, respectively, in the B6 mice and by 35% and 41%, respectively, in the β-gal$^{-/-}$ mice. Furthermore, *N*B-DGJ significantly reduced cerebellar GD3 content by ~50% in the B6 mice and by ~44% in the β-gal$^{-/-}$ mice (Table 2). Other gangliosides (GD1a, GT1a/LD1, GD1b, and GT1b) were also reduced in either the C-BS or the cerebellum of the *N*B-DGJ-treated B6 and β-gal$^{-/-}$ mice (Table 2). In contrast to most other gangliosides, *N*B-DGJ had no significant effect on C-BS or cerebellar GQ1b content in either the normal or the mutant mice.

The qualitative distribution of neutral lipids in the C-BS and cerebellum of p-15 B6 and β-gal$^{-/-}$ mice is shown in **Fig. 3**. *N*B-DGJ had no obvious effect on the content or distribution of neutral lipids, including cholesterol, ceramide, cerebrosides, phosphatidylethanolamine, phosphatidylcholine, and GA1, in the C-BS and cerebellum of the B6 and β-gal$^{-/-}$ mice. The cerebrosides migrated as prominent double bands on the chromatogram and were more heavily expressed in cerebellum than in the C-BS. Sphingomyelin content in the C-BS and in the cerebellum was significantly increased by 42% and 12%, respectively, in the treated B6 mice, and by 31% and 18%, respectively, in the β-gal$^{-/-}$ mice (**Table 3**). Also, sphingomyelin content was generally higher in the cerebellum than in the C-BS of the normal and mutant mice. Although absent in the normal B6 CNS, GA1 accumulated in the CNS of the β-gal$^{-/-}$ mice, and accumulation was greater in the C-BS than in the cerebellum (Table 3). *N*B-DGJ treatment had no significant effect on GA1 content in either brain region. Cerebrosides in the B6 mice and cerebrosides and GA1 in the β-gal$^{-/-}$ mice were the only neutral GSLs detectable in the C-BS or cerebellum.

To determine whether ganglioside synthesis inhibition influenced cerebellar development, we examined cerebellar morphology and the thickness of the EGL in control and *N*B-DGJ-treated β-gal$^{-/-}$ mice (**Fig. 4**). Cerebellar morphology was similar in the control and treated β-gal$^{-/-}$ mice. Also, no differences were found between the control and treated β-gal$^{-/-}$ mice for EGL thickness in vernal lobule VI (14.5 ± 0.4 and 13.7 ± 0.6 μm, respectively) or in vernal lobule X (20.3 ± 1.3 and 19.6 ± 1.1 μm, respectively). These data indicate that *N*B-DGJ treatment does not alter granule cell migration in the cerebellum and are consistent with behavioral evidence that *N*B-DGJ does not alter ambulation or righting reflex. Additionally, cerebellar morphology and EGL thickness were similar in untreated B6 and β-gal$^{-/-}$ mice at p-15.

DISCUSSION

In our previous study, we showed that *N*B-DGJ could significantly reduce total brain and GM1 content when

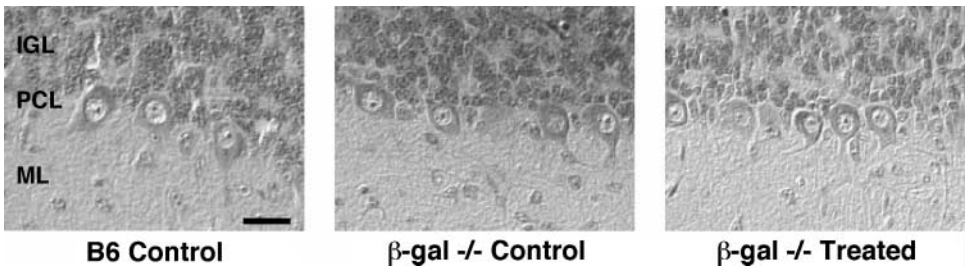

Fig. 1. Luxol Fast Blue staining of vernal lobule III of the cerebellum in postnatal day 15 (p-15) C57BL/6J (B6) and β-galactosidase knockout (β-gal$^{-/-}$) mice. The mice were injected daily from p-9 to p-15 with either saline (control) or 600 mg/kg *N*-butyldeoxygalactonojirimycin (*N*B-DGJ; treated). Purkinje cell cytoplasm of either the control or the treated β-gal$^{-/-}$ mice was similar to that of the B6 mice with no evidence of neuronal vacuoles. IGL, internal granular layer; ML, molecular layer; PCL, Purkinje cell layer. Scale bar = 25 μm.

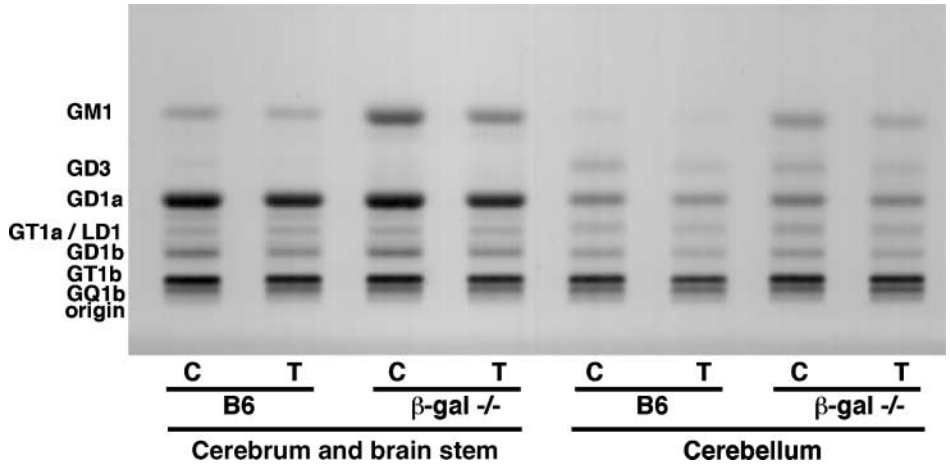

Fig. 2. High-performance thin-layer chromatography (HPTLC) distribution of brain and cerebellum gangliosides in postnatal (p-15) normal B6 and mutant β-gal$^{-/-}$ mice. The mice were injected daily from p-9 to p-15 with either saline (C) or 600 mg/kg *N*B-DGJ (T). The amount of ganglioside sialic acid spotted per lane was equivalent to ~0.75 mg of tissue dry weight. The plate was developed by a single ascending run with $CHCl_3$/CH_3OH/deionized H_2O (dH_2O) (55:45:10, v/v) containing 0.02% $CaCl_2 \cdot 2H_2O$. The bands were visualized with resorcinol-HCl spray.

administered from p-2 to p-5 in control B6 and mutant β-gal$^{-/-}$ mice (3). The p-2 to p-5 neonatal ages in mice are comparable to prenatal ages in humans as they precede the period of active brain myelinogenesis and cerebellar development. Moreover, the reduction in CNS ganglioside content had no adverse effects on development. It was not known from this study, however, whether *N*B-DGJ treatment could also be effective at older ages, especially during critical stages of cerebellar development and myelinogenesis. No previous studies have examined the effects of this drug on CNS lipids during these developmental ages. It was also not known whether the neonatal mice could tolerate *N*B-DGJ injections for 7 days during this critical period. In the present study, we found that *N*B-DGJ treatment from p-9 to p-15 significantly reduced total ganglioside and GM1 content both in the C-BS and in the developing cerebellum of normal B6 and mutant β-gal$^{-/-}$ mice, indicating a CNS-wide effect. Moreover, these reductions in ganglioside content had no obvious adverse effects on behavior or CNS development.

We found that *N*B-DGJ significantly reduced total ganglioside and GD3 content in the cerebellum of β-gal$^{-/-}$ mice without altering morphology or the thickness of the EGL. GD3 is enriched in vertebrate CNS neuroectodermal cells, including granule cells of the EGL, in the developing mouse cerebellum (29, 47–53). Our findings indicate that inhibition of total ganglioside and GD3 biosynthesis did not affect the migration of granule cells from the EGL to the internal granular layer. These observations are consistent with previous findings that *N*B-DGJ-induced inhibition of ganglioside biosynthesis does not impair brain development in the organogenesis-stage mouse embryo (27). Hence, *N*B-DGJ may be an effective early intervention therapy for ganglioside storage diseases during critical stages of brain development.

The amount of myelin in the brain is directly propor-

TABLE 2. Regional brain ganglioside distribution in p-15 normal B6 and mutant β-gal$^{-/-}$ mice treated with *N*B-DGJ

Brain Region	Strain	Treatment[a]	Concentration[b]						
			GM1	GD3	GD1a	GT1a/LD1	GD1b	GT1b	GQ1b
			μg sialic acid/100 mg dry wt						
Brain[c]	B6	Control	31.2 ± 2.1	3.9 ± 0.4	235.5 ± 3.3	13.4 ± 1.3	45.7 ± 6.3	135.3 ± 2.9	36.6 ± 1.3
		Treated	25.7 ± 2.8	3.1 ± 0.5	202.3 ± 11.3[d]	12.2 ± 1.8	36.4 ± 1.0	104.3 ± 10.5[d]	37.6 ± 3.3
	β-Gal$^{-/-}$	Control	117.3 ± 3.6	Trace	190.0 ± 2.4	12.4 ± 1.9	69.1 ± 4.5	137.7 ± 2.8	61.1 ± 5.1
		Treated	76.2 ± 3.5[e]	Trace	162.8 ± 9.2[d]	11.9 ± 0.9	52.0 ± 1.7[d]	117.7 ± 3.9[d]	57.5 ± 1.5
Cerebellum	B6	Control	10.8 ± 0.3	38.7 ± 3.2	78.4 ± 5.8	22.8 ± 2.5	27.6 ± 1.6	125.5 ± 10.2	37.9 ± 9.8
		Treated	9.0 ± 0.4[d]	19.3 ± 1.7[e]	63.7 ± 7.3	18.7 ± 4.1	14.9 ± 3.2[d]	98.0 ± 11.8	42.6 ± 6.9
	β-Gal$^{-/-}$	Control	54.7 ± 1.7	28.3 ± 1.9	63.8 ± 1.3	21.5 ± 0.6	28.8 ± 1.1	112.6 ± 4.6	50.5 ± 0.3
		Treated	32.0 ± 0.4[e]	15.9 ± 1.1[e]	58.7 ± 1.6[d]	17.4 ± 1.0[d]	19.8 ± 1.2[e]	95.1 ± 0.7[d]	48.8 ± 1.0

Values represent means ± SEM of three independent samples.
[a] Mice were injected daily with either vehicle (control) or *N*B-DGJ (treated) at 600 mg/kg from p-9 to p-15.
[b] Determined from densitometric scanning of high-performance thin-layer chromatographs as shown in Fig. 1.
[c] Region includes cerebrum + brain stem.
[d] Significantly different from control values at $P < 0.05$ (determined from the two-tailed *t*-test).
[e] Significantly different from control values at $P < 0.01$ (determined from the two-tailed *t*-test).

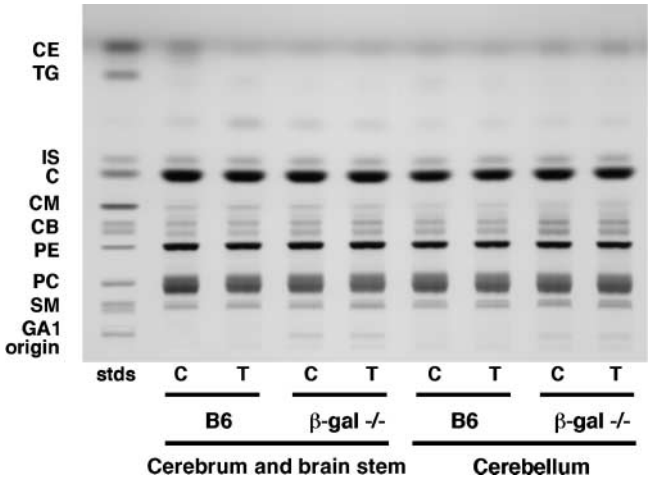

Fig. 3. HPTLC of brain and cerebellum neutral lipids in postnatal (p-15) normal B6 and mutant β-gal$^{-/-}$ mice. The mice were injected daily from p-9 to p-15 with either saline (C) or 600 mg/kg *N*B-DGJ (T). The amount of neutral lipids spotted per lane was equivalent to ~0.3 mg of tissue dry weight. The plate was developed to a height of 4.5 cm with chloroform-methanol-acetic acid-formic acid-water (35:15:6:2:1, v/v), then developed to the top with hexanes-diisopropyl ether-acetic acid (65:35:2, v/v). The bands were visualized by charring with 3% cupric acetate in 8% phosphoric acid solution. C, cholesterol; CB, cerebrosides (doublet); CE, cholesteryl esters; CM, ceramide; GA1, asialo GM1; IS, internal standard (oleyl alcohol); PC, phosphatidylcholine; PE, phosphatidylethanolamine; SM, sphingomyelin; stds, lipid standards; TG, triglycerides.

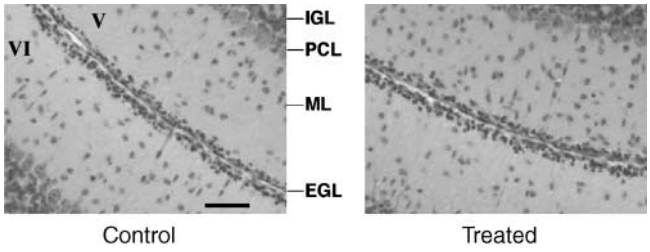

Fig. 4. Hematoxylin and eosin staining of the cerebellum between vernal lobules V and VI in p-15 β-gal$^{-/-}$ mice. The mice were injected daily from p-9 to p-15 with either saline (control) or 600 mg/kg *N*B-DGJ (treated). External granular layer (EGL) thickness was similar in the control and the treated mice (see Results). IGL, internal granular layer; ML, molecular layer; PCL, Purkinje cell layer. Scale bar = 50 μm.

tional to the concentration of cerebroside, a neutral GSL (30, 45, 54). Myelination also occurs earlier in cerebellum than in cerebral cortex according to phylogenetic development (36). We previously showed that the rate of cerebroside accumulation was greatest in B6 mice from p-14 to p-16 (30). In addition to cerebroside, GM1 is also enriched in mammalian CNS myelin (30, 55–58). The amount of water in the brain is another factor associated with CNS myelin content, because myelin is dehydrated relative to gray matter (30, 36, 59). Therefore, it would be important to determine whether ganglioside synthesis inhibition and GM1 reduction influenced myelinogenesis in normal and mutant mice. The prominent cerebroside doublet seen on HPTLC in both the C-BS and cerebellum is indicative of active myelinogenesis in the p-15 brains. Our data show that the content of CNS cerebrosides and water was not altered after *N*B-DGJ treatment in either B6 or β-gal$^{-/-}$ mice. These findings suggest that *N*B-DGJ treatment does not adversely affect myelinogenesis in the developing mouse CNS.

Ceramide, sphingomyelin, and cerebroside are sphingolipids that could be influenced by *N*B-DGJ treatment (3, 27, 60). We previously found increases of whole brain ceramide and sphingomyelin in neonatal mice treated with a high *N*B-DGJ concentration (1,200 mg/kg) from p-2 to p-5 (3). In the present study, we found that sphingomyelin was the only CNS neutral lipid significantly increased in the p-15 treated mice. The sphingomyelin increase might be a compensatory response to an increase of ceramide that we observed previously in mice treated from p-2 to p-5 (3). This would be reasonable, because ceramide is a precursor for sphingomyelin synthesis. Moreover, it would be important to maintain low levels of ceramide because ceramide has been implicated in neural cell apoptosis (27, 61). *N*B-DGJ treatment had no significant effect on the distribution of other major CNS neutral lipids. These findings, viewed together with the ganglioside analysis, suggest that *N*B-DGJ primarily reduces ganglioside content and has little effect on most major CNS neutral lipids. We do not exclude the possibility that *N*B-DGJ might influence the CNS distribution of minor neutral GSLs (e.g., glucosylceramide, lactosylceramide, or globoside), but these lipids were undetectable in either the C-BS or the cerebellum.

Extensive CNS storage of PAS-positive material and neuronal vacuoles occurs by ~5 weeks of age in the β-gal$^{-/-}$ mice (2). Previous studies with another β-gal$^{-/-}$ mouse model showed CNS storage material between 2 and 3 weeks of age (62). Despite significant increases of GM1, we were unable to detect neuronal vacuoles or lipid storage material in either the C-BS or the cerebellum using LFB or PAS in p-15 β-gal$^{-/-}$ mice. These findings indicate that biochemical ganglioside accumulation in this mouse model has not reached the point of clear histological detection

TABLE 3. Regional brain sphingomyelin and GA1 content in p-15 normal B6 and mutant β-gal$^{-/-}$ mice treated with *N*B-DGJ

		Sphingomyelin		GA1	
Strain	Treatment[a]	Brain[b]	Cerebellum	Brain	Cerebellum
		μg/100 mg dry wt			
B6	Control	325 ± 25	465 ± 12	—	—
	Treated	460 ± 31[c]	522 ± 10[c]	—	—
β-Gal$^{-/-}$	Control	422 ± 17	503 ± 15	259 ± 17	167 ± 14
	Treated	552 ± 2[d]	596 ± 15[c]	272 ± 16	157 ± 10

GA1, asialo GM1. Values represent means ± SEM of three independent samples.

[a] Mice were injected daily with either vehicle (control) or *N*B-DGJ (treated) at 600 mg/kg from p-9 to p-15.

[b] Region includes cerebrum + brain stem.

[c] Significantly different from control values at $P < 0.05$ (determined from the two-tailed *t*-test).

[d] Significantly different from control values at $P < 0.01$ (determined from the two-tailed *t*-test).

by p-15. Consequently, it was not possible to determine if *N*B-DGJ treatment could reduce CNS storage material or neuronal vacuoles. Based on our current findings and those of our previous study in p-5 mice, we suggest that *N*B-DGJ could be used to target ganglioside accumulation during the entire period of postnatal development. Further studies in older mutant mice that were treated throughout development could determine whether the *N*B-DGJ-induced reductions in CNS GM1 content are associated with reductions in CNS storage material and neuronal vacuoles.

In contrast to our previous findings in mutant β-gal$^{-/-}$ mice at p-5, *N*B-DGJ treatment did not increase CNS GA1 content in the mutants at p-15. A lower *N*B-DGJ concentration used in this study (600 mg/kg vs. the 1,200 mg/kg used in the previous study) may account for the difference. It is also important to note that CNS GA1 content is proportionally greater in the mouse than in the human forms of the disease, possibly as a result of a more active sialidase in the mouse (2, 63, 64). Assuming that CNS GA1 in the mutant mouse is derived largely from GM1 desialylation, it is interesting that *N*B-DGJ treatment, which reduced GM1 content, did not also reduce GA1 content. Recent studies showed that *N*B-DGJ could enhance lysosomal enzyme activity through chaperone effects (7, 65). Further studies will be needed to assess possible *N*B-DGJ chaperone effects and the relationship between GM1, GA1, and sialidase activity in the control and *N*B-DGJ-treated β-gal$^{-/-}$ mice.

In summary, our results show that *N*B-DGJ reduces C-BS and cerebellar total ganglioside and GM1 content in normal B6 and β-gal$^{-/-}$ mice during critical stages of CNS development. Moreover, these ganglioside reductions had no observable adverse effects on behavior or CNS development. These findings, together with our previous observations in p-5 mice, suggest that *N*B-DGJ may be an effective early intervention therapy for ganglioside storage diseases and should have translational benefit to the clinic.

This work was supported by the Boston College Research Expense Fund, grants from the National Institutes of Health (HD-39722) and the National Tay-Sachs and Allied Disease Association, Inc., and the Burroughs Wellcome Fund. The authors thank Rena Baek, Christine Denny, and Lisa Mahoney for technical assistance.

REFERENCES

1. Suzuki, Y., H. Sakuraba, and A. Oshima. 1995. β-Galactosidase deficiency (β-galactosidosis): GM1 gangliosidosis and Morquio B disease. *In* The Metabolic and Molecular Bases of Inherited Disease. C. R. Scriver, A. L. Beaudet, W. S. Sly, and D. Valle, editors. McGraw-Hill, Inc., New York. 2785–2823.
2. Hahn, C. N., M. del Pilar Martin, M. Schroder, M. T. Vanier, Y. Hara, K. Suzuki, K. Suzuki, and A. d'Azzo. 1997. Generalized CNS disease and massive GM1-ganglioside accumulation in mice defective in lysosomal acid beta-galactosidase. *Hum. Mol. Genet.* **6:** 205–211.
3. Kasperzyk, J. L., M. M. El-Abbadi, E. C. Hauser, A. D'Azzo, F. M. Platt, and T. N. Seyfried. 2004. N-Butyldeoxygalactonojirimycin reduces neonatal brain ganglioside content in a mouse model of GM1 gangliosidosis. *J. Neurochem.* **89:** 645–653.
4. Dobrenis, K. 2004. Cell-mediated delivery systems. *In* Lysosomal Disorders of the Brain. F. M. Platt and S. U. Walkley, editors. Oxford University Press, New York. 339–380.
5. Lacorazza, H. D., J. D. Flax, E. Y. Snyder, and M. Jendoubi. 1996. Expression of human beta-hexosaminidase alpha-subunit gene (the gene defect of Tay-Sachs disease) in mouse brains upon engraftment of transduced progenitor cells. *Nat. Med.* **2:** 424–429.
6. Norflus, F., C. J. Tifft, M. P. McDonald, G. Goldstein, J. N. Crawley, A. Hoffmann, K. Sandhoff, K. Suzuki, and R. L. Proia. 1998. Bone marrow transplantation prolongs life span and ameliorates neurologic manifestations in Sandhoff disease mice. *J. Clin. Invest.* **101:** 1881–1888.
7. Matsuda, J., O. Suzuki, A. Oshima, Y. Yamamoto, A. Noguchi, K. Takimoto, M. Itoh, Y. Matsuzaki, Y. Yasuda, S. Ogawa, Y. Sakata, E. Nanba, K. Higaki, Y. Ogawa, L. Tominaga, K. Ohno, H. Iwasaki, H. Watanabe, R. O. Brady, and Y. Suzuki. 2003. Chemical chaperone therapy for brain pathology in GM1-gangliosidosis. *Proc. Natl. Acad. Sci. USA.* **100:** 15912–15917.
8. Schiffmann, R., and R. O. Brady. 2002. New prospects for the treatment of lysosomal storage diseases. *Drugs.* **62:** 733–742.
9. Takaura, N., T. Yagi, M. Maeda, E. Nanba, A. Oshima, Y. Suzuki, T. Yamano, and A. Tanaka. 2003. Attenuation of ganglioside GM1 accumulation in the brain of GM1 gangliosidosis mice by neonatal intravenous gene transfer. *Gene Ther.* **10:** 1487–1493.
10. Tropak, M. B., S. P. Reid, M. Guiral, S. G. Withers, and D. Mahuran. 2004. Pharmacological enhancement of beta-hexosaminidase activity in fibroblasts from adult Tay-Sachs and Sandhoff patients. *J. Biol. Chem.* **279:** 13478–13487.
11. Brady, R. O. 2003. Enzyme replacement therapy: conception, chaos and culmination. *Philos. Trans. R. Soc. Lond. B Biol. Sci.* **358:** 915–919.
12. Radin, N. S. 1982. Inhibitors and stimulators of glucocerebroside metabolism. *Prog. Clin. Biol. Res.* **95:** 357–383.
13. Platt, F. M., and T. D. Butters. 2004. Inhibition of substrate synthesis: a pharmacological approach for glycosphingolipid storage disease therapy. *In* Lysosomal Disorders of the Brain. F. M. Platt and S. U. Walkley, editors. Oxford University Press, New York. 381–408.
14. Tifft, C. J., and R. L. Proia. 2000. Stemming the tide: glycosphingolipid synthesis inhibitors as therapy for storage diseases. *Glycobiology.* **10:** 1249–1258.
15. Butters, T. D., H. R. Mellor, K. Narita, R. A. Dwek, and F. M. Platt. 2003. Small-molecule therapeutics for the treatment of glycolipid lysosomal storage disorders. *Philos. Trans. R. Soc. Lond. B Biol. Sci.* **358:** 927–945.
16. Liu, Y. Y., T. Y. Han, A. E. Giuliano, and M. C. Cabot. 1999. Expression of glucosylceramide synthase, converting ceramide to glucosylceramide, confers adriamycin resistance in human breast cancer cells. *J. Biol. Chem.* **274:** 1140–1146.
17. Andersson, U., D. Smith, M. Jeyakumar, T. D. Butters, M. C. Borja, R. A. Dwek, and F. M. Platt. 2004. Improved outcome of N-butyldeoxygalactonojirimycin-mediated substrate reduction therapy in a mouse model of Sandhoff disease. *Neurobiol. Dis.* **16:** 506–515.
18. Vunnam, R. R., and N. S. Radin. 1980. Analogs of ceramide that inhibit glucocerebroside synthetase in mouse brain. *Chem. Phys. Lipids.* **26:** 265–278.
19. Butters, T. D., R. A. Dwek, and F. M. Platt. 2003. Therapeutic applications of imino sugars in lysosomal storage disorders. *Curr. Top. Med. Chem.* **3:** 561–574.
20. Platt, F. M., M. Jeyakumar, U. Andersson, T. Heare, R. A. Dwek, and T. D. Butters. 2003. Substrate reduction therapy in mouse models of the glycosphingolipidoses. *Philos. Trans. R. Soc. Lond. B Biol. Sci.* **358:** 947–954.
21. Platt, F. M., and S. U. Walkley, editors. 2004. Lysosomal Disorders of the Brain. Oxford University Press, New York.
22. Platt, F. M., G. R. Neises, G. Reinkensmeier, M. J. Townsend, V. H. Perry, R. L. Proia, B. Winchester, R. A. Dwek, and T. D. Butters. 1997. Prevention of lysosomal storage in Tay-Sachs mice treated with N-butyldeoxynojirimycin. *Science.* **276:** 428–431.
23. Cox, T. M., J. M. Aerts, G. Andria, M. Beck, N. Belmatoug, B. Bembi, R. Chertkoff, S. Vom Dahl, D. Elstein, A. Erikson, M. Giralt, R. Heitner, C. Hollak, M. Hrebicek, S. Lewis, A. Mehta, G. M. Pastores, A. Rolfs, M. C. Miranda, and A. Zimran. 2003. The role of the iminosugar N-butyldeoxynojirimycin (miglustat) in the management of type I (non-neuronopathic) Gaucher disease: a position statement. *J. Inherit. Metab. Dis.* **26:** 513–526.
24. Lachmann, R. H. 2003. Miglustat. Oxford GlycoSciences/Actelion. *Curr. Opin. Invest. Drugs.* **4:** 472–479.

25. Kolodny, E. H., O. Neudorfer, J. Gianutsos, C. Zaroff, N. Barnett, B. Zeng, S. Raghavan, P. Torres, and G. Pastores. 2004. Late-onset Tay-Sachs disease: natural history and treatment with OGT 918. *J. Neurochem.* **90 (Suppl. 1):** 54.
26. Andersson, U., T. D. Butters, R. A. Dwek, and F. M. Platt. 2000. N-Butyldeoxygalactonojirimycin: a more selective inhibitor of glycosphingolipid biosynthesis than N-butyldeoxynojirimycin, in vitro and in vivo. *Biochem. Pharmacol.* **59:** 821–829.
27. Brigande, J. V., F. M. Platt, and T. N. Seyfried. 1998. Inhibition of glycosphingolipid biosynthesis does not impair growth or morphogenesis of the postimplantation mouse embryo. *J. Neurochem.* **70:** 871–882.
28. Muse, E. D., H. Jurevics, A. D. Toews, G. K. Matsushima, and P. Morell. 2001. Parameters related to lipid metabolism as markers of myelination in mouse brain. *J. Neurochem.* **76:** 77–86.
29. Seyfried, T. N., N. Miyazawa, and R. K. Yu. 1983. Cellular localization of gangliosides in the developing mouse cerebellum: analysis using the weaver mutant. *J. Neurochem.* **41:** 491–505.
30. Seyfried, T. N., and R. K. Yu. 1980. Heterosis for brain myelin content in mice. *Biochem. Genet.* **18:** 1229–1238.
31. Matthieu, J. M., S. Widmer, and N. Herschkowitz. 1973. Biochemical changes in mouse brain composition during myelination. *Brain Res.* **55:** 391–402.
32. Verbitskaya, L. B. 1969. Some aspects of ontophylogenesis of the cerebellum. *In* Neurobiology of Cerebellar Evolution and Development. R. Llinas, editor. Institute for Biomedical Research AMA/ERF, Chicago. 859–874.
33. Morell, P., and R. H. Quarles. 1999. Myelin formation, structure and biochemistry. *In* Basic Neurochemistry. G. J. Siegel, B. W. Agranoff, R. W. Albers, S. K. Fisher, and M. D. Uhler, editors. Lippincott-Raven, New York. 69–93.
34. Galjaard, H., editor. 1980. Genetic Metabolic Disease: Diagnosis and Prenatal Analysis. Elsevier Science Publishers, Amsterdam.
35. Hauser, E. C., J. L. Kasperzyk, A. d'Azzo, and T. N. Seyfried. 2004. Inheritance of lysosomal acid b-galactosidase activity and gangliosides in crosses of DBA/2J and knockout mice. *Biochem. Genet.* **42:** 241–257.
36. Seyfried, T. N., G. H. Glaser, and R. K. Yu. 1978. Cerebral, cerebellar, and brain stem gangliosides in mice susceptible to audiogenic seizures. *J. Neurochem.* **31:** 21–27.
37. Macala, L. J., R. K. Yu, and S. Ando. 1983. Analysis of brain lipids by high performance thin-layer chromatography and densitometry. *J. Lipid Res.* **24:** 1243–1250.
38. Folch, J., M. Lees, and G. H. Sloane-Stanley. 1957. A simple method for the isolation and purification of total lipids from animal tissues. *J. Biol. Chem.* **226:** 497–509.
39. Svennerholm, L. 1957. Quantitative estimation of sialic acids. II. A colorimetric resorcinol-hydrochloric acid method. *Biochim. Biophys. Acta.* **24:** 604–611.
40. Miettinen, T., and I. T. Takki-Luukkainen. 1959. Use of butyl acetate in the determination of sialic acid. *Acta Chem. Scand. A.* **13:** 856–858.
41. Suzuki, K. 1964. A simple and accurate micromethod for quantitative determination of ganglioside patterns. *Life Sci.* **3:** 1227–1233.
42. Williams, M. A., and R. H. McCluer. 1980. The use of Sep-Pak C18 cartridges during the isolation of gangliosides. *J. Neurochem.* **35:** 266–269.
43. Ando, S., N. C. Chang, and R. K. Yu. 1978. High-performance thin-layer chromatography and densitometric determination of brain ganglioside compositions of several species. *Anal. Biochem.* **89:** 437–450.
44. Bruckner, J. 1955. Estimation of monosaccharides by the orcinol-sulphuric acid reaction. *Biochem. J.* **60:** 200–205.
45. Seyfried, T. N., D. Bernard, F. Mayeda, L. Macala, and R. K. Yu. 1984. Genetic analysis of cerebellar lipids in mice susceptible to audiogenic seizures. *Exp. Neurol.* **84:** 590–595.
46. Seyfried, T. N., R. K. Yu, and N. Miyazawa. 1982. Differential cellular enrichment of gangliosides in the mouse cerebellum: analysis using neurological mutants. *J. Neurochem.* **38:** 551–559.
47. Seyfried, T. N., D. J. Bernard, and R. K. Yu. 1984. Cellular distribution of gangliosides in the developing mouse cerebellum: analysis using the staggerer mutant. *J. Neurochem.* **43:** 1152–1162.
48. Seyfried, T. N. 1987. Ganglioside abnormalities associated with failed neural differentiation in a T-locus mutant mouse embryo. *Dev. Biol.* **123:** 286–291.
49. Irvine, R. A., and T. N. Seyfried. 1994. Phylogenetic conservation of ganglioside GD3 expression during early vertebrate ontogeny. *Comp. Biochem. Physiol. B Biochem. Mol. Biol.* **109:** 603–612.
50. Rosner, H., M. al-Aqtum, and H. Rahmann. 1992. Gangliosides and neuronal differentiation. *Neurochem. Int.* **20:** 339–351.
51. Schaal, H., C. Wille, and W. Wille. 1985. Changes of ganglioside pattern during cerebellar development of normal and staggerer mice. *J. Neurochem.* **45:** 544–551.
52. Goldman, J. E., M. Hirano, R. K. Yu, and T. N. Seyfried. 1984. GD3 ganglioside is a glycolipid characteristic of immature neuroectodermal cells. *J. Neuroimmunol.* **7:** 179–192.
53. Goldman, J. E., and R. Reynolds. 1996. A reappraisal of ganglioside GD3 expression in the CNS. *Glia.* **16:** 291–295.
54. Norton, W. T., and S. E. Poduslo. 1973. Myelination in rat brain: method of myelin isolation. *J. Neurochem.* **21:** 749–757.
55. Ebato, H., T. N. Seyfried, and R. K. Yu. 1983. Biochemical study of heterosis for brain myelin content in mice. *J. Neurochem.* **40:** 440–446.
56. Yu, R. K., and S. I. Yen. 1975. Gangliosides in developing mouse brain myelin. *J. Neurochem.* **25:** 229–232.
57. Suzuki, K., J. F. Poduslo, and W. T. Norton. 1967. Gangliosides in the myelin fraction of developing rats. *Biochim. Biophys. Acta.* **144:** 375–381.
58. Yu, R. K., and K. Iqbal. 1979. Sialosylgalactosyl ceramide as a specific marker for human myelin and oligodendroglial perikarya: gangliosides of human myelin, oligodendroglia and neurons. *J. Neurochem.* **32:** 293–300.
59. Norton, W. T. 1977. Isolation and characterization of myelin. *In* Myelin. P. Morell, editor. Plenum, New York. 161–199.
60. Platt, F. M., G. Reinkensmeier, R. A. Dwek, and T. D. Butters. 1997. Extensive glycosphingolipid depletion in the liver and lymphoid organs of mice treated with N-butyldeoxynojirimycin. *J. Biol. Chem.* **272:** 19365–19372.
61. Wiesner, D. A., and G. Dawson. 1996. Staurosporine induces programmed cell death in embryonic neurons and activation of the ceramide pathway. *J. Neurochem.* **66:** 1418–1425.
62. Itoh, M., J. Matsuda, O. Suzuki, A. Ogura, A. Oshima, T. Tai, Y. Suzuki, and S. Takashima. 2001. Development of lysosomal storage in mice with targeted disruption of the beta-galactosidase gene: a model of human G(M1)-gangliosidosis. *Brain Dev.* **23:** 379–384.
63. Sango, K., S. Yamanaka, A. Hoffmann, Y. Okuda, A. Grinberg, H. Westphal, M. P. McDonald, J. N. Crawley, K. Sandhoff, K. Suzuki, et al. 1995. Mouse models of Tay-Sachs and Sandhoff diseases differ in neurologic phenotype and ganglioside metabolism. *Nat. Genet.* **11:** 170–176.
64. Riboni, L., A. Caminiti, R. Bassi, and G. Tettamanti. 1995. The degradative pathway of gangliosides GM1 and GM2 in Neuro2a cells by sialidase. *J. Neurochem.* **64:** 451–454.
65. Tominaga, L., Y. Ogawa, M. Taniguchi, K. Ohno, J. Matsuda, A. Oshima, Y. Suzuki, and E. Nanba. 2001. Galactonojirimycin derivatives restore mutant human beta-galactosidase activities expressed in fibroblasts from enzyme-deficient knockout mouse. *Brain Dev.* **23:** 284–287.

ERRATA

In the article "Substrate reduction reduces gangliosides in postnatal cerebrum-brainstem and cerebellum in GM1 gangliosidosis mice" by Kasperzyk et al., published in the April 2004 issue of the *Journal of Lipid Research* (Volume **46**, pages 744–751), the affiliations should read as follows:

J. L. Kasperzyk,* A. d'Azzo,† F. M. Platt,§ J. Alroy,** and T. N. Seyfried*,[1]

Department of Biology,* Boston College, Chestnut Hill, MA; Department of Genetics,† St. Jude Children's Research Hospital, Memphis, TN; Glycobiology Institute,§ Department of Biochemistry, University of Oxford, Oxford, United Kingdom; and Department of Pathology,** Tufts University School of Medicine and Veterinary Medicine, New England Medical Center, Boston, MA

[1]To whom correspondence should be addressed.
e-mail: thomas.seyfried@bc.edu

*****

In the article "Prediction of PPAR-α ligand-mediated physiological changes using gene expression profiles" by Frederiksen et al., published in the March 2004 issue of the *Journal of Lipid Research* (Volume **45**, pages 592–601), the digital object identifier (DOI) should read: DOI 10.1194/jlr.M300239-JLR200.

*****

In the article "Regulation of ganglioside biosynthesis in the nervous system" by Yu et al., published in the May 2004 issue of the *Journal of Lipid Research* (Volume **45**, pages 783–793), the digital object identifier (DOI) should read: DOI 10.1194/jlr.R300020-JLR200.

*****

In the article "Cholesterol metabolism in the central nervous system during early development and in the mature animal" by Dietschy and Turley, published in the August 2004 issue of the *Journal of Lipid Research* (Volume **45**, pages 1375–1397), the digital object identifier (DOI) should read: DOI 10.1194/jlr.R400004-JLR200.